PAPER • OPEN ACCESS

Microwave assisted synthesis of zinc vanadate nanoparticles and photocatalytic application

To cite this article: M Iqbal *et al* 2020 *Mater. Res. Express* **7** 015070

Materials Research Express

OPEN ACCESS

RECEIVED
25 October 2019

REVISED
29 December 2019

ACCEPTED FOR PUBLICATION
8 January 2020

PUBLISHED
20 January 2020

PAPER

Microwave assisted synthesis of zinc vanadate nanoparticles and photocatalytic application

M Iqbal[1], M Fatima[1], T Javed[2], A Anam[1], A Nazir[1,8], Q Kanwal[1], Z Shehzadi[3], M I Khan[4], J Nisar[5], M Abbas[6] and S Naz[7,8]

[1] Department of Chemistry, The University of Lahore, Lahore 53700, Pakistan
[2] Department of Chemistry, University of Sahiwal, Sahiwal, Pakistan
[3] Government College Women University Sialkot, Sialkot, Pakistan
[4] Department of Physics, The University of Lahore, Lahore 53700, Pakistan
[5] National Center of Excellence in Physical Chemistry, University of Peshawar, Peshawar 25120, Pakistan
[6] Department of Basic Sciences, College of Veterinary and Animal Sciences, Jhang Campus, UVAS, Lahore, Pakistan
[7] Department of Chemistry, Division of Science and Technology, University of Education, Multan Campus, Pakistan
[8] Authors to whom any correspondence should be addressed.

E-mail: anmalik77@gmail.com **and** saima.naz@ue.edu.pk

Keywords: synthesis, characterization, zinc vanadate, photocatalytic activity, degradation, microwave assisted

Abstract

In recent years, the nanotechnology has gained much attention since the nanoparticles (NPs) have applications in every field of life. The hetero-structured are of special interest due to their higher photocatalytic activity. In present investigation, Zinc vanadate NPs were synthesized from vanadium and zinc salts by microwave assisted precipitation method. The Zinc vanadate NPs were characterized by x-ray Powder Diffraction (XRD), Energy-dispersive x-ray spectroscopy (EDX), Scanning electron microscope (SEM) and UV-visible techniques. The photocatalytic activity (PCA) was evaluated by degrading the methylene blue (MB) dye and process variables were optimized. The Zinc vanadate size was <100 nm and particles were in aggregates form. The MB dye degradation was performed at different conditions of process variables and it was observed that MB dye was significantly degraded using Zinc vanadate NPs under UV light irradiation. The reaction time, catalyst dose and dye initial concentration showed variable effect on dye degradation. Based on results, it can be concluded that the microwave irradiation is viable for the synthesis of Zinc vanadate NPs for photocatalytic activity. In view of promising efficiency of Zinc vanadate NPs, it can be used for the dye degradation and for the remediation of textile effluents.

1. Introduction

Metal oxide play pivotal role in material science and can adopt various structural geometries with electronic distribution that exhibit metallic or semiconductor character. The semiconductor pure and doped metal oxide properties depend on their morphology, structure and grain size [1, 2]. Metal oxide nanoparticles have been used in electroanalysis and detection of biomolecules. The nanoparticles are useful with respect to structural changes that allow the changes in symmetry and cell parameters. On the other hand, the changes in electrochemical characteristics and in surface properties increase the band gap that effects the chemical activity of the nanoparticles [3, 4]. So far, these materials have the ability to improve the properties and have enormous applications in many fields such asmicroelectronics, batteries, sensing device, nano probes and nano medicine. Nanostructure of vanadium oxide (VO) have been studied [5–8] and a variety of nanostructures in the form of 1D to 3D of V_2O_5 have been preferred as a model system for the depiction of nanostructured materials. One of the major applications of VO is lithium ion batteries. These NPs are usually prepared via hydrothermal heating of aqueous solution [9, 10]. Nano wires, nano belts or nano-urchin shapes are synthesized by chemical parameters which depends on the arrangement of a VO network that act as a precursor in synthesized nanotubes and nanorods [11–14].

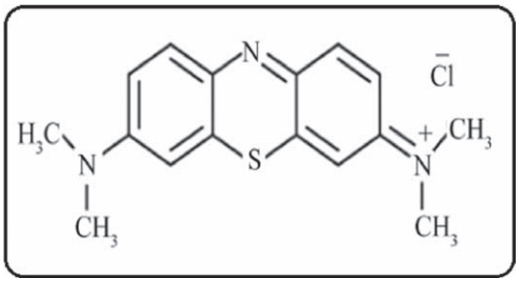

Figure 1. Structure of methylene Blue (MB) dye.

Various strategies i.e. immobilized TiO_2, non-thermal plasma, Pt deposited TiO_2 films, TiO_2 nano fibers, bismuth degradation have been successfully employed for degradation of pharmaceuticals in wastewater [14–16]. The most common use of semiconductor photo catalysis is to control pollution. Under the UV light irradiation these oxides degrade the organic pollutants [17–20].

The VO act as the catalyst with band gap around 2.6 eV. These active band have an arrow gap makes in a wide region of UV light frequencies approaches are frequently implemented. Different parameters of nanomaterials application have been used for food safety and food packing such as silver NPs as potent antimicrobial agent, polymer/clay nano composites as high barrier packaging materials, nanomaterial, nano-sensors based assays for the detection of food-relevant analytes. With various compositions NPs have been preparedby physical and chemical methods. The physical methods may be evaporation, sputtering, laser ablation, ion ejection, and electron- beam lithography [15, 16, 21].

The chemical methods consist of a salt reduction method, micelles, electrochemical sol-gel method, gas-liquid interface, thermolysis and decomposition on ultrasonic treatment. They improved the energy efficiency of photo generated supported various composition for appropriate co-catalysts. The atavistic has been improved at which the photocatalytic reaction occurs in which electrons moves to the holes from bulk to reaction active sites [22–27].

However, in view of the drawbacks faced by low efficiency, instability, semiconductor pure oxides in photocatalytic process, researchers are now focusing on the synthesis of nano hetero-structured photo catalysts [28–31]. Moreover, owing to their robust nature and versatility in morphology, the hetero-structured NPs show better performance as photo-catalysts and are gaining attention of scientific community [32, 33]. Zinc vanadate and their derivatives have also been investigated for extensive chemical sensing, lubrication cathode materials catalysis and plating [18, 20, 34].

More recently, $Zn_3(VO_4)_2$ nano rods with visible light-driven capacity were prepared by hydrothermal method. The degradation of MB and 4-nitrophenol over the $Zn_3(VO_4)_2$ nano rods were reported, which was synthesized by hydrothermal route. As-synthesized 3D Zinc vanadate nanoflower was characterized by XRD, SEM, AFM, EDX, Particle size and UV–vis techniques. Moreover, PCA was evaluated for the degradation of cetirizine hydrochloride (C-HCl) using RSM under CCD [35, 36].

The reports concerning the crystal growth and dimension control of Zinc vanadate without any template under microwave irradiation are rare. Therefore, the present study was conducted for the synthesis of Zinc vanadate under microwave irradiation. The synthesized Zinc vanadate was characterized by SEM, XRD, EDX, UV–vis techniques. Moreover, the PCA was evaluated for the degradation of methyl blue dye (figure 1).

2. Materials and methods

All the chemicals and reagents employed in this study were of analytical grade and were purchased from Sigma-Aldrich. Ultra-pure water (resistivity18.2 Mohm.com) was obtained from Milli-Q plant. Standard stock solution of each required reagents was prepared by dilution method. Desired concentrations were obtained from stock solution [37].

2.1. Synthesis procedure

For the synthesis, ammonium vanadate and $ZnCl_2$ solutions was prepared and mixed with each other at 85 °C under continuous stirring. Then, solution was divided into two parts. One was heated on magnetic hot plate, other under microwave treatment and ammonium hydroxide was added for pH adjustment of the solution. The pH was adjusted 8.8 and then content in the beaker was left over night at 85 °C to allow the precipitates to settle

down. Solvent was decanted and precipitates was washed with ultra-pure water followed by ethanol washing (thrice) to ensure the removal of unreacted ions and then, calcined at 500 °C for 5 h [38, 39].

2.2. Characterization

In order to characterize the Zinc vanadate catalyst different characterization techniques were used. For shape and morphology (structure) of catalyst, scanning electron microscopy was performed using SEM (JSM-5910, JEOL). For elemental analysis, Energy Dispersive x-ray Spectroscopy (EDX) was used. For crystal size and phase, XRD (JDX-3532) was used [40].

2.3. Photocatalytic activity

The PCA was evaluated under UV light irradiation using low pressure mercury lamps. For the photolysis and photocatalysis of aqueous solution of MB dye, a photochemical apparatus fitted with a 4W low pressure Hg-UV lamp (PENARY USA) was used. The wavelength of the emitted light by Hg-UV lamp was 254 nm. A magnetic stirrer was used for stirring the sample to achieve homogenous flow of UV radiation throughout the solution [41].

The MB dye solutions of different concentrations were prepared in ultra–pure water and catalyst was added at specific ratios. In order to dissolve the catalyst, sonication was carried out for 10 min. To achieve the adsorption-desorption equilibrium, dark stirring was carried out for 30 min. Sample of dark stirring were collected and analyzed to get the spectra. The UV light irradiated samples were collected at different times and filtered through micro syringe filter. Then the remaining concentration of MB dye was determined by spectrophotometric analysis. All the experiments were performed in a glass beaker of 250 ml. Specific quantity of catalyst powder was mixed with 50 mL of MB dye solution. The pH of the solution was adjusted using acid base solution. The solution in the beaker was sonicated for 10 min and then continuously for 30 min in dark for the establishment of adsorption-desorption equilibrium. To quantify the degradation, 3 mL of sample was collected at specific time from the reactor, filtered through 0.22 mm micro syringe filters and then, analyzed through UV spectrophotometer (CE Cecil 7200 UK). The percent of MB dye degradation was measured using relation shown in equation (1).

$$\text{Degradation of MB dye (\%)} = \left[\frac{C_0 - C_i}{C_0}\right] \times 100 \quad (1)$$

Where, C_0 and C_i are the initial concentration of MB dye and the concentration at different time intervals, respectively. All the samples were irradiated in triplicate and data was averaged and reported as mean ±standard deviation.

3. Results and discussion

In recent years, the nanotechnology has gained much attention since the nanoparticles (NPs) have huge applications in every field of life. The hetero-structured NPs are of special interest due their higher photocatalytic activity [42, 43]. In present investigation, Zinc vanadate NPs were synthesized from vanadium and zinc salts by microwave assisted precipitation method. The Zinc vanadate NPs were characterized by XRD, EDX, SEM, UV–visible techniques. The particles were round in shape and size of synthesized material was 100 nm.

The XRD pattern (0–80°) of synthesized zinc vanadate is shown in figure 2. XRD analysis exhibited the formation of pure form of Zinc vanadate and well indexed with JCPDS card (50–0570). This study seizures the direct precipitation approach for the synthesis of 3-D spherical Zinc vanadate flower. The synthesized Zinc vanadate was in pure phase hexagonal form. Peaks obtained at sharp edges reflect the higher crystallinity of the compound without any impurity peak.

The morphology was determined with SEM and results are shown figure 3 and 4. The Zinc vanadate was first formed in small particle (nano range), then these were combined to form aggregates. The microwave treated effect was also significant since the morphology was changed as the samples were irradiated with microwave. The composition of Zinc vanadate was confirmed by EDX analysis and results are shown in figure 5. The EDX spectrum shows peaks related to Zinc vanadate and no additional peak was observed, which indicate the adopted method was used sucessfuly for the synthesis of Zinc vanadate. The EDX revealed the presence of V(21.22%), O(19.85%), Zn(58.93%) and the atomic percentages were 16.28%, 48.49% and 35.23%. These results are in line with reported study for Zinc vanadate, for example, Timmaji [44] synthesized $BiVO_4$ by solution combustion synthesis and electrodeposition. The first deposition of Bi film on a Pt substrate in an acidic $BiCl_3$ medium. This film anodically exposed those medium that contain hydrolyzed vanadium precursor to produce Bi^{3+} and subsequent $BiVO_4$ formation by *in situ* precipitation. Glycine, citric acid, urea was used at the same time as the fuel. The probe of Methyl orange was used to test the combustion synthesized (CS) samples and photocatalytic

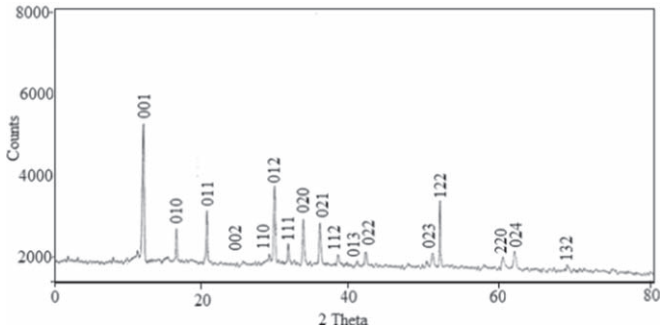

Figure 2. XRD analysisof zinc vanadate without microwave irradiation.

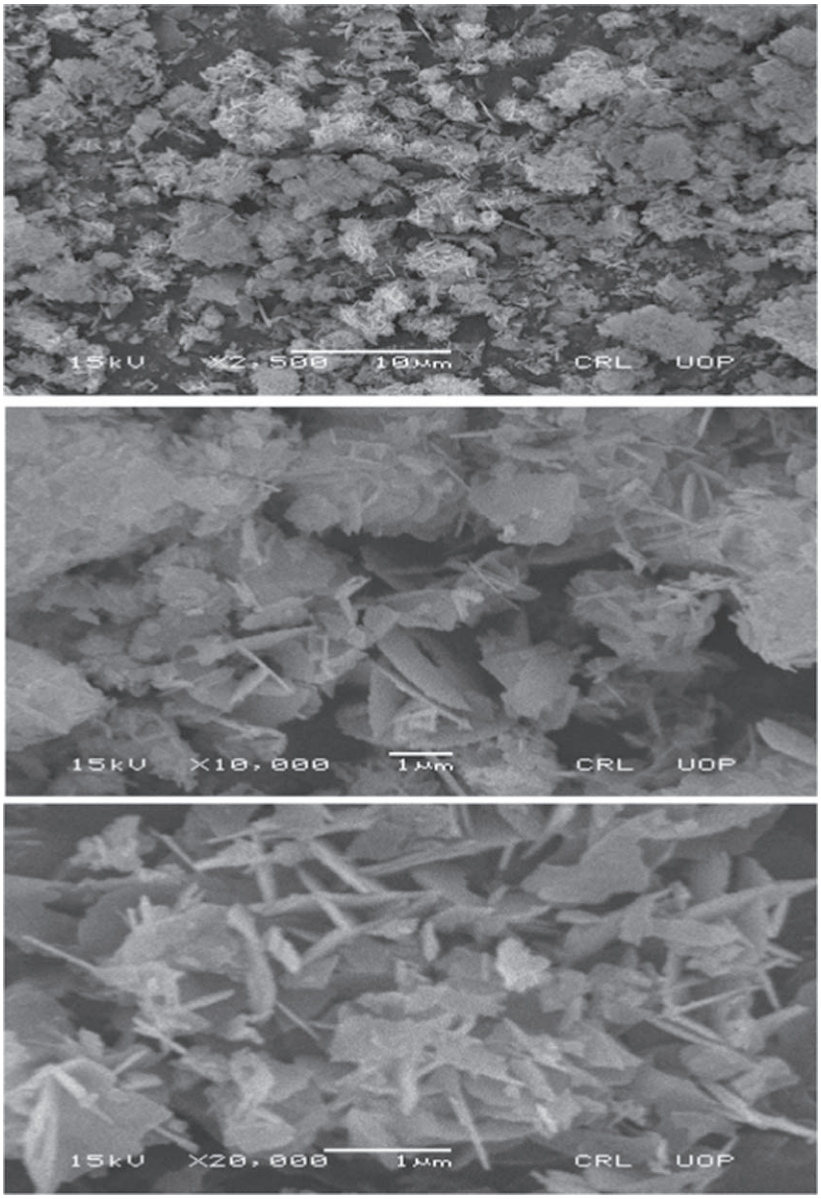

Figure 3. SEM images of zinc vanadate NPs under microwave irradiation.

attributes.The nanoparticles ($AgBiW_2O_8$) were prepared for the first time by solution combustion analysis via bismuth nitrate sodium tungstate, silver nitrate as precursors for Bi, Ag and W correspondingly and urea used as the fuel. Similarly, Ibrahim, Khan [45] synthesized nanoflakes $WO_3/BiVO_4$ hterojuncation prepared by facile hydrothermal method.

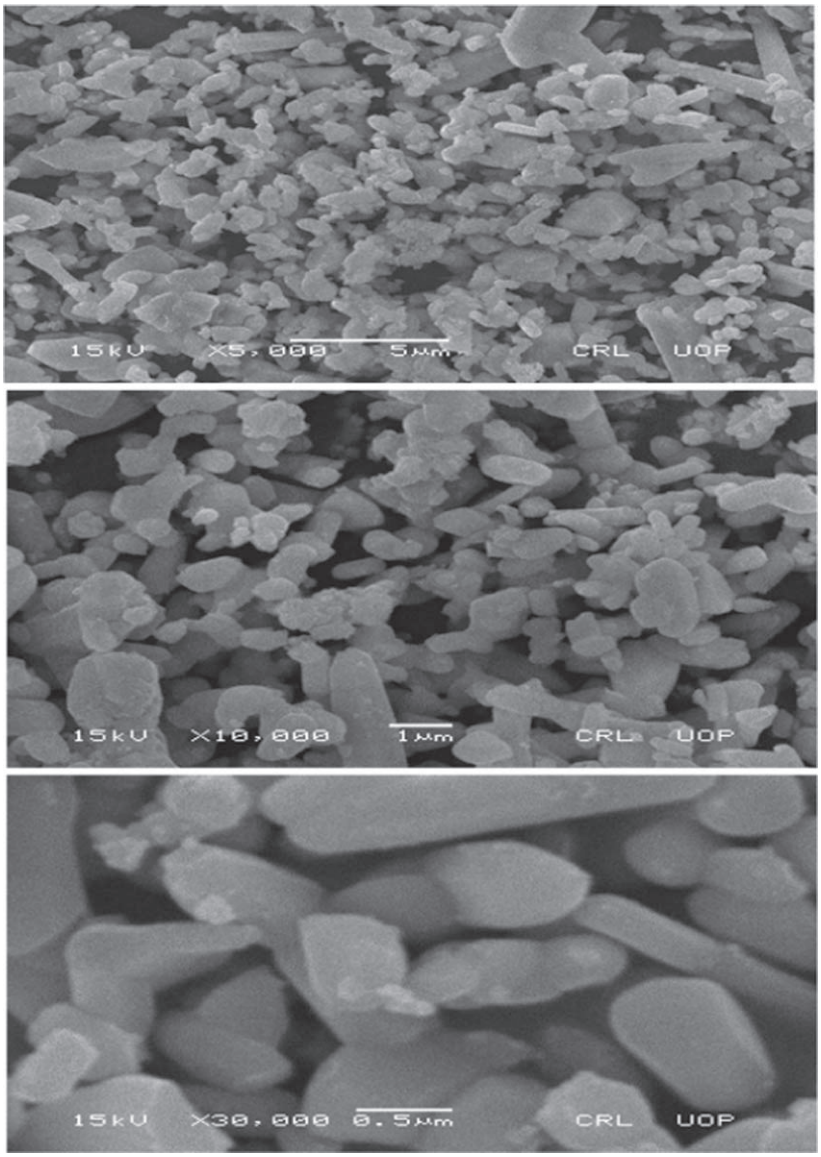

Figure 4. SEM images of zinc vanadate NPs without microwave irradiation.

3.1. Photocatalytic studies

3.1.1. Effect of exposure time of PCA

The influence of different reaction times on decolorization efficiency of MB dye is illustrated in figure 6. The first order linear relationship was revealed by the plots of the (C/C_0) vs. irradiation time (t), where C was the concentration of MB dye at the irradiation time (t) and C_0 was the concentration before irradiation. When time interval is increased from 0 to 80 min the decolorization efficiency of dye also increases from 0 to 66% and then complete degradation occurs at 160 min. The interaction of catalyst with UV light increases which is indicative of the fact that active sites of the catalyst increased which further enhance the production of highly reactive species. This confirms that activity of catalyst increases with time. The data revealed that the degradation efficiency of the dye increased with extending irradiation time. Absorbance of the solution at 554 nm with time was determined to monitor the MB dye concentration. The decrease in the concentration of MB dye with time was due to its degradation by catalyst. It can be seen that in about 3 h, almost all the MB dye was degraded. So, time of 160 min was selected for further study. The same MB dye was degraded by Mahadik, Shinde [46] who studied the Fe_2O_3 as a photocatalyst, but they obtained low degradation efficiency for longer reaction time. So the prepared catalyst was very active by degrading the MB dye up to 83% in 160 min, [47] prepared (m-$BiVO_4$) photocatalytic and antimicrobial activity was studied. Photocatalytic activity of m-$BiVO_4$ nanostructure was evaluated by degrading the MB dye, which is a waste of textiles industries.

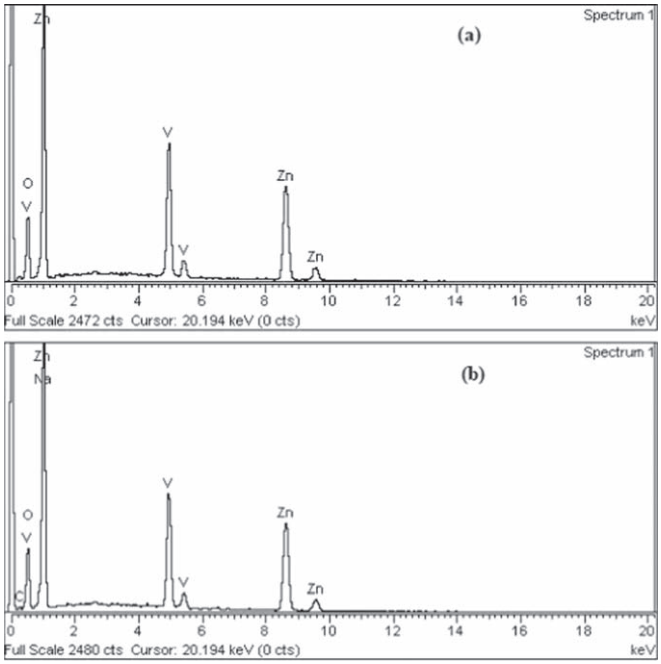

Figure 5. EDX of zinc vanadate (a) under microwave irradiation and (b) without microwave irradiation.

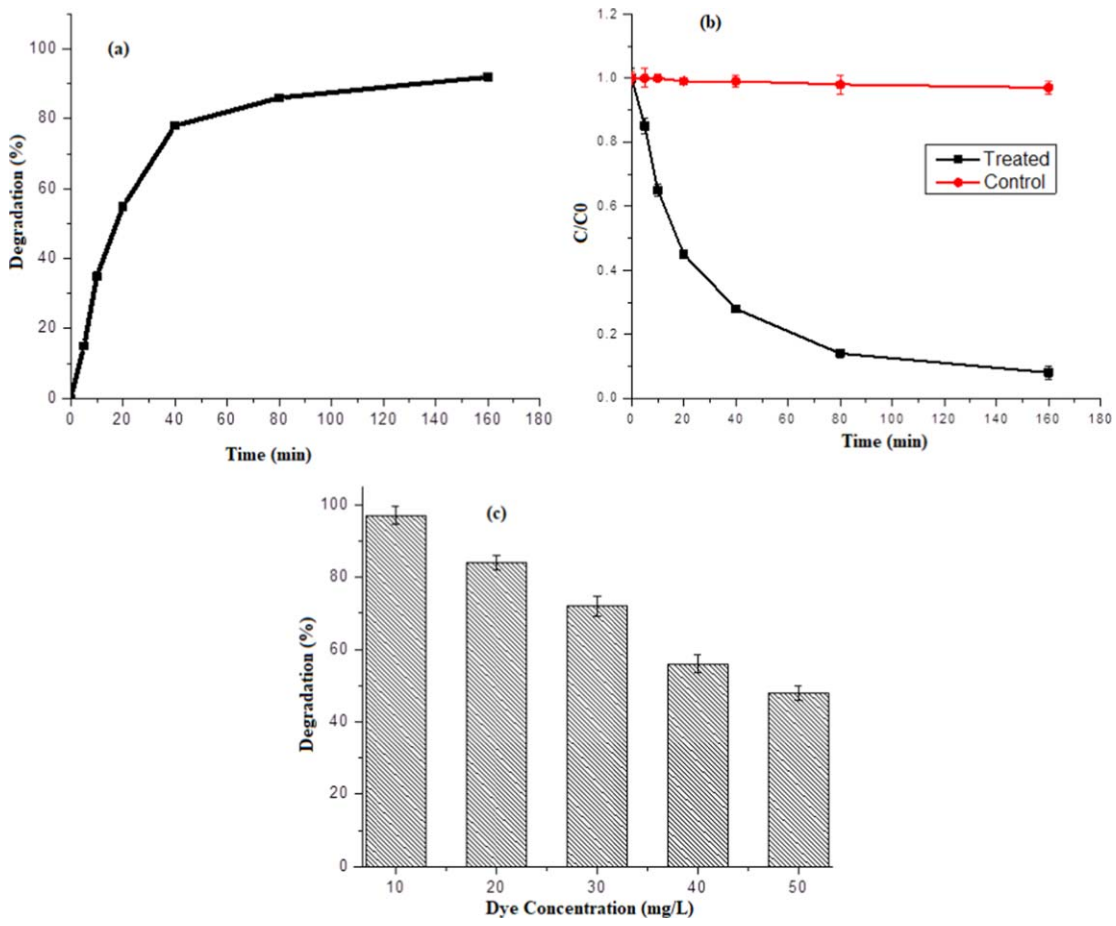

Figure 6. (a) Graphical presentation of percentage degradation of MB dye as a function of time, (b) Rate plots showing activity of zinc vanadate and (c) MB dye degradation at different initial concentrations of dye.

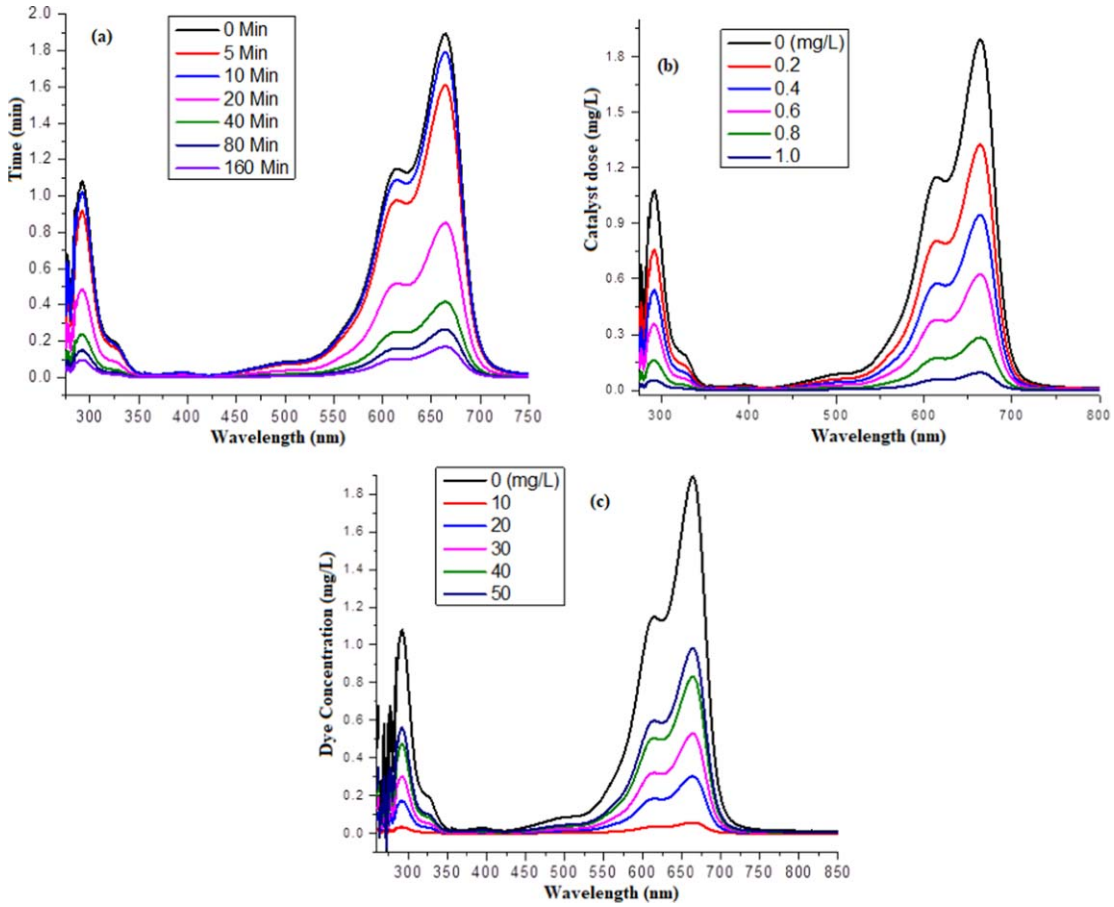

Figure 7. UV-visible spectra of dye degradation (a) as afunction of time, (b) as afunction of catalyst dose and (c) at different dye initial concentration.

3.1.2. Effect of catalyst dose

In order to evaluate the photocatalytic degradation of the MB dye under UV light, blank experiment was performed. The first order linear relationship was revealed by the plots of the (C/C_0) vs. catalyst dose (figure 7). The rate of degradation process is negligible when experiment was carried out in the absence of catalyst. It suggests that the catalyst must be used in combination with UV light for the degradation of dye. The degradation of the MB dye increased when ZnV_2O_8 catalyst dose was increased. This indicates that the degradation of MB dye increases in the presence of photocatalyst. The increase in degradation rate may be attributed to the production of highly reactive oxidizing species and high generation of free radicals by catalyst in the presence of UV light which degraded the dye to a large extent [48–53]. Under these experimental conditions, and after 10 min of UV irradiation, the degradation reaches 83% of MB dye. The concentration of MB dye in the solution was also mentioned spectrophotometrically by measuring the absorbance of the solution at 665 nm. After ascertaining the activity shown by the as synthesized ZnV_2O_8 the effective parameters were selected for further study. Also, [16] evaluated the photodegradation efficiency of BiVO4 and graphene oxide (RGO) composite. The photocatalysts RGO-BiVO4 show high degradation efficiency versus pure BiVO4 photocatalyst under visible light. Specially, composite photocatalyst of the 2 wt. % RGO-$BiVO_4$ exhibits the highest CIP degradation ratio (68.2%) in 60 min, which is over 3 times than that (22.7%) of the pure $BiVO_4$ particles. However, the catalysts which act as active site and play a role as proton donors in the photodegradation process of the organic compounds due to higher surface area.

3.1.3. Effect of dye concentration

Solutions of different dye concentrations (10, 20, 30, 40, 50 mg l^{-1}) were prepared. The absorbance spectra of the solutions of different concentrations were carried out and their respective corresponding maximum absorbance were noted (Figure. 7). All the absorbance data were recorded at 665 nm which is the maximum corresponding absorbance wavelength of MB dye. A graph of absorbance versus different concentrations was plotted. Graph shows that with the increase in dye concentration, the degradation was decreased. Also, [54] prepared BiOCl/$BiVO_4$ photocatalyst with heterojunction structure using a hydrothermal method. Under visible light irradiations, the heterojunction have been

suggested for the degradation of methyl orange (MO).The photocatalytic efficiency for MO photodegradation was increased versus BiOCl, $BiVO_4$ and Degussa P_{25}.This activity has been obtained usingheterojunction composite of 13 mol % BiOCl and 87 mol % $BiVO_4$.The removal of MO has been mainly initiated by consuming the conduction band electrons valence-band holes that play important role in photocatalytic activity. Wang, Shao [55] also synthesized novel BiOCl–C_3N_4 heterojunctions through-liquid-assisted solvent-thermal method. UV–visible light diffusion reflectance spectrometry was performed. These results show that they are dispersed to form heterojunction structures to absorb visible light. The methyl orange (MO) degradation indicated heterojunction proportion that increased the visible light absorption for photocatalytic activity.

4. Conclusions

In present investigation, Zinc vanadate NPs were synthesized from vanadium and zinc salts by microwave assisted precipitation method. The Zinc vanadate NPs were characterized by XRD, EDX, SEM, UV-vis. techniques. The Zinc vanadate size was <100 nm and particles were in aggregates form. The MB dye degradation was performed at different conditions of process variables and it was observed that MB dye was significantly degraded using Zinc vanadate NPs under UV light irradiation. The reaction time, catalyst dose and dye initial concentration showed variable effect on dye degradation. Based on results, it can be concluded that the microwave irradiation is viable for the synthesis of Zinc vanadate NPs for photocatalytic application. In view of promising efficiency of Zinc vanadate NPs, it can be used for the degradation of dye and for the remediation of other industrial pollutants present in wastewater.

ORCID iDs

M Iqbal https://orcid.org/0000-0001-7393-8065
A Nazir https://orcid.org/0000-0002-9412-6100

References

[1] Josephine B A *et al* 2016 Fundamental study of $LaMg_xCr_{1-x}O_{3-\delta}$ perovskites nano-photocatalysts: sol-gel synthesis, characterization and humidity sensing *Korean J. Chem. Eng.* **33** 1590–8
[2] Suguna S *et al* 2018 Novel synthesis and characterization studies of spinel $Ni_xCo_{1-x}Al_2O_4$ (x = 0.0 to 1.0) nano-catalysts for the catalytic oxidation of benzyl alcohol *J. Nanosci. Nanotechnol.* **18** 1019–26
[3] Algarou N *et al* 2019 Enhancement on the exchange coupling behavior of SrCo0. 02Zr0. 02Fe11. 96O19/MFe_2O_4 (M = Co, Ni, Cu, Mn and Zn) as hard/soft magnetic nanocomposites. *J. Magnet. Magnet. Mater.* **499** 166308
[4] Racik M *et al* 2019 Hydrothermal synthesis and characterization studies of α-Fe_2O_3/MnO_2 nanocomposites for energy storage supercapacitor application *Ceram. Int.* (https://doi.org/10.1016/j.ceramint.2019.11.091)
[5] Gholami Shiri Z, Zebarjad S M and Janghorban K 2019 A study on the role of electrospinning parameters on the morphology of nickel oxide nano-belts *Mater. Res. Exp.* **6** 1150a8
[6] Abu El-Fadl A, Nashaat A M and Kassem M A 2019 Characterization of spinel-type $Cd_{1-x}Co_xCr_2O_4$ nanocrystals by a microwave-combustion synthesis *Mater. Res. Exp.* **6** 1150a7
[7] Shang L *et al* 2019 Growth behavior of β-Ga_2O_3 nanowires synthesized by chemical vapor deposition *Mater. Res. Exp.* **6** 1150a5
[8] Abu-Dief A M and Mohamed W S 2017 α-Bi_2O_3 nanorods: synthesis, characterization and UV-photocatalytic activity *Mater. Res. Exp.* **4** 035039
[9] Chen Z *et al* 2009 Preparation and electrochemical performance of Sn–Co–C composite as anode material for Li-ion batteries *J. Power Sour.* **189** 730–2
[10] Ulucan-Altuntas K and Kuzu S L 2019 Modelling and optimization of dye removal by Fe/Cu bimetallic nanoparticles coated with different Cu ratios *Mater. Res. Exp.* **6** 1150a4
[11] Chen Z *et al* 2016 Preparation of nickel cobalt sulfide hollow nanocolloids with enhanced electrochemical property for supercapacitors application *Sci. Rep.* **6** 25151
[12] John A A *et al* 2017 Folic acid decorated chitosan nanoparticles and its derivatives for the delivery of drugs and genes to cancer cells *Curr. Sci.* **113** 1530
[13] Vellayappan M, Jaganathan S and Manikandan A 2016 Nanomaterials as a game changer in the management and treatment of diabetic foot ulcers *RSC Adv.* **6** 114859–78
[14] Thema F *et al* 2016 Single phase Bunsenite NiO nanoparticles green synthesis by Agathosma betulina natural extract *J. Alloy. Comp.* **657** 655–61
[15] Subramanian A *et al* 2016 Recent trends in nano-based drug delivery systems for efficient delivery of phytochemicals in chemotherapy *RSC Adv.* **6** 48294–314
[16] Kasinathan K *et al* 2016 Photodegradation of organic pollutants RhB dye using UV simulated sunlight on ceria based TiO(2) nanomaterials for antibacterial applications *Sci. Rep.* **6** 38064–38064
[17] Zhang Z, Hossain M F and Takahashi T 2010 Photoelectrochemical water splitting on highly smooth and ordered TiO2 nanotube arrays for hydrogen generation *Int. J. Hyd. Ener.* **35** 8528–35
[18] Awwad A M *et al* 2020 Green synthesis, characterization of silver sulfide nanoparticles and antibacterial activity evaluation *Chem. Int.* **6** 42–8
[19] Alasadi M, Khaili F I and Awwad A M 2019 Adsorption of Cu(II), Ni(II) and Zn(II) ions by nano kaolinite: Thermodynamics and kinetics studies *Chem. Int.* **5** 258–68

[20] Igwe O and Nwamezie F 2018 Green synthesis of iron nanoparticles using flower extract of Piliostigma thonningii and antibacterial activity evaluation *Chem. Int.* **4** 60–6
[21] John A A *et al* 2016 Surface modification of titanium and its alloys for the enhancement of osseointegration in orthopaedics *Curr. Sci.* **111** 1003
[22] Kamran U *et al* 2019 Green synthesis of metal nanoparticles and their applications in different fields: a review *Z. Phys. Chem.* **233** 1325–49
[23] Hussain A *et al* 2019 Investigating the antibacterial activity of POMA nanocomposites *Pol. J. Environ. Stud.* **28** 4191–8
[24] Aal R M A, Gitru M A and Essam Z M 2017 Novel synthetized near infrared cyanine dyes as sensitizer for dye sensitized solar cells based on nano-TiO_2 *Chem. Int.* **3** 358–67
[25] Cahyana A H and Kam N 2016 Study on the stability of antioxidant and anti α-glucosidase activities using soaking treatment in Okra (Abelmoschus esculentus L.) mucilage extraction *Chem. Int.* **3** 202–11
[26] Jamal M A, Muneer M and Iqbal M 2015 Photo-degradation of monoazo dye blue 13 using advanced oxidation process *Chem. Int.* **1** 12–6
[27] Elvia R, Cahyana A H and Wibowo W 2015 Catalytic acetylation of (+)-cedrol with heterogeneous catalyst H_2SO_4/SiO_2 under solvent free conditions *Chem. Int.* **1** 196–201
[28] Vanitha D *et al* 2018 Studies on conducting polymer blends: synthesis and characterizations of PVA/PVP doped with $CaCl_2$ *J. Nanosci. Nanotechnol.* **18** 1723–9
[29] Sundaramahalingam K *et al* 2018 Studies on sodium nitrate based polyethylene oxide/polyvinyl pyrrolidone polymer blend electrolytes *Phys. B: Cond. Matt.* **547** 55–63
[30] Silambarasu A *et al* 2018 Comparative study of structural, morphological, magneto-optical and photo-catalytic properties of magnetically reusable spinel $MnFe_2O_4$ nano-catalysts *J. Nanosci. Nanotechnol.* **18** 3523–31
[31] Bomila R *et al* 2018 Enhanced photocatalytic degradation of methylene blue dye, opto-magnetic and antibacterial behaviour of pure and La-doped ZnO nanoparticles *J. Supercond. Nov. Magnet.* **31** 855–64
[32] Silambarasu A, Manikandan A and Balakrishnan K 2017 Room-temperature superparamagnetism and enhanced photocatalytic activity of magnetically reusable spinel $ZnFe_2O_4$ nanocatalysts *J. Supercond. Nov. Magnet.* **30** 2631–40
[33] Shameem A *et al* 2017 Preparation and characterization studies of nanostructured CdO thin films by SILAR method for photocatalytic applications *J. Inorg. Organomet. Polym. Mater.* **27** 692–9
[34] Arshad M *et al* 2018 Influence of different solvents on portrayal and photocatalytic activity of tin-doped zinc oxide nanoparticles *J. Mol. Liq.* **260** 272–8
[35] Bibi I *et al* 2019 Structural, dielectric and magnetic studies of perovskite [$Gd_{1-x}M_xCrO_3$ (M = La, Co, Bi)] nanoparticles: photocatalytic degradation of dyes *Z. Phys. Chem.* 1431–45
[36] Arshad M *et al* 2018 Zn-doped SiO_2 nanoparticles preparation and characterization under the effect of various solvents: Antibacterial, antifungal and photocatlytic performance evaluation *J. Photochem. Photobiol. B: Biol.* **185** 176–83
[37] Zhao Y *et al* 2008 Surfactant-free synthesis of hyperbranched monoclinic bismuth vanadate and its applications in photocatalysis, gas sensing, and lithium-ion batteries *Chem. Eur. J.* **14** 1601–6
[38] Majid F *et al* 2019 Hydrothermal synthesis of zinc doped nickel ferrites: evaluation of structural, magnetic and dielectric properties *Z. Phys. Chem.* **233** 1411–30
[39] Nazar N *et al* 2018 Cu nanoparticles synthesis using biological molecule of P. granatum seeds extract as reducing and capping agent: growth mechanism and photo-catalytic activity *Int. J. Biol. Macromol.* **106** 1203–10
[40] Bibi I *et al* 2017 Nickel nanoparticle synthesis using Camellia Sinensis as reducing and capping agent: Growth mechanism and photo-catalytic activity evaluation *Int. J. Biol. Macromol.* **103** 783–90
[41] Bibi I *et al* 2017 Green and eco-friendly synthesis of cobalt-oxide nanoparticle: characterization and photo-catalytic activity *Adv. Powder Technol.* **28** 2035–43
[42] Senthil R A *et al* 2019 One-pot preparation of AgBr/α-Ag_2WO_4 composite with superior photocatalytic activity under visible-light irradiation *Coll. Surf. A: Physicochem. Eng. Asp.* **586** 124079
[43] Babitha N *et al* 2019 Enhanced antibacterial activity and photo-catalytic properties of ZnO nanoparticles: pedalium murex plant extract-assisted synthesis *J. Nanosci. Nanotechnol.* **19** 2888–94
[44] Timmaji H K 2012 *Bismuth-Based oxide Semiconductors: mild Synthesis and Practical Applications* **253** 41–58
[45] Ibrahim A A *et al* 2017 Facile synthesis of tungsten oxide–bismuth vanadate nanoflakes as photoanode material for solar water splitting *Int. J. Hyd. Ener.* **42** 3423–30
[46] Mahadik M *et al* 2014 Visible light catalysis of rhodamine B using nanostructured Fe2O3, TiO2 and TiO2/Fe2O3 thin films *J. Photochem. Photobiol. B: Biol.* **133** 90–8
[47] Sharma R *et al* 2016 Visible light induced bactericidal and photocatalytic activity of hydrothermally synthesized BiVO4 nano-octahedrals *J. Photochem. Photobiol. B: Biol.* **162** 266–72
[48] Ghezali S *et al* 2018 Adsorption of 2, 4, 6-trichlorophenol on bentonite modified with benzyldimethyltetradecylammonium chloride *Chem. Int.* **4** 24–32
[49] Legrouri K *et al* 2017 Activated carbon from molasses efficiency for Cr (VI), Pb (II) and Cu (II) adsorption: a mechanistic study *Chem. Int.* **3** 301–10
[50] Igwe O U and Friday C 2017 Volatile constituents of hydrocolloids isolated from Afzelia africana and Detarium microcarpum seeds. *Chem. Int.* **3** 286–91
[51] Arshad R *et al* 2020 Gamma radiation induced degradation of anthraquinone Reactive Blue-19 dye using hydrogen peroxide as oxidizing agent *Radiat. Phys. Chem.* **168** 108637
[52] Qureshi N *et al* 2019 Synthesis of fluorescent di-dansyl substituted ethoxy compound: A selective sensor for antimony and thallium metals detection *J. Mater. Res. Technol.* **8** 1576–80
[53] Khan N U H *et al* 2019 Decolorization of basic turquise blue X-GB and basic blue X-GRRL by the Fenton's Process and its Kinetics *Z. Phys. Chem.* **233** 361–73
[54] Fan H *et al* 2012 Effect of $BiVO_4$ crystalline phases on the photoinduced carriers behavior and photocatalytic activity *The J. Phys. Chem. C.* **116** 2425–30
[55] Wang F *et al* 2009 The synthesis of monoclinic bismuth vanadate nanoribbons and studies of photoconductive, photoresponse, and photocatalytic properties *Mater. Res. Bull.* **44** 1687–91